Fusion Engineering and Design 88 (2013) 1844–1847

Contents lists available at ScienceDirect

Fusion Engineering and Design

journal homepage: www.elsevier.com/locate/fusengdes

Thermal analysis of the Mirnov coils of Wendelstein 7-X

M.Y. Ye [a,d,*], X.B. Peng [b,c], L. Fransico [b], M. Endler [b]

[a] School of Nuclear Science and Technology, University of Science and Technology of China, Jinzhai Road 96, 230026 Hefei, Anhui, PR China
[b] Max Planck Institute for Plasma Physics, EURATOM Association, Wendelsteinstr. 1, 17491 Greifswald, Germany
[c] Institute of Plasma Physics, Chinese Academy of Sciences, Shushanhu Road 350, 230031 Hefei, Anhui, PR China
[d] Collaborative Innovation Center for Advanced Fusion energy & Plasma Science, University of Science and Technology of China, Jinzhai Road 96, 230026 Hefei, Anhui, PR China

ARTICLE INFO

Article history:
Received 14 September 2012
Received in revised form 1 May 2013
Accepted 23 May 2013
Available online 18 June 2013

Keywords:
W7-X
Mirnov coil
Steady state
Transient
Thermal analysis

ABSTRACT

Mirnov coils are used to measure fluctuations of the magnetic field which are in particular generated by magnetohydrodynamic (MHD) modes. The underlying plasma currents have a multipolar structure in a poloidal cross-section. Therefore the amplitude of the magnetic fluctuations decays quickly with increasing distance from the plasma edge. It is hence important to place the Mirnov coils as close to the plasma edge as possible where they are exposed to high thermal loads. Two types of Mirnov coils are proposed to be used in Wendelstein 7-X (W7-X). Type 1 (44 Mirnov coils) should be mounted on the plasma side of wall protection panels with a graphite cap to shield them from direct plasma exposure. Type 2 (137 Mirnov coils) will be located behind the tiles of the heat shields. An important issue concerning the design of these Mirnov coils is to verify their suitability for steady state operation from the thermal point of view. Both steady state and transient finite element thermal analyses were performed for the Mirnov coils under different conditions and with different designs. The paper presents detailed thermal analyses of the Mirnov coils.

1. Introduction

The superconducting stellarator W7-X, being under construction in Greifswald by Max-Plank-Institut für Plasmaphysik (IPP), is designed for stationary operation (30 min) with 10 MW continuous wave heating by electron cyclotron resonance heating (ECRH), and additional 14 MW heating by ion cyclotron resonance heating (ICRH) and neutral beam injection (NBI) for 10 s. The plasma facing components (PFCs) are designed to withstand radiative and/or conventional heat loads in the range of 100 kW/m^2 to 10 MW/m^2 [1–3] and have a basic function to protect the components behind them from direct plasma exposure. However, diagnostic components located behind the PFCs need further active cooling due to the significant thermal radiation coming from the cooled but still rather hot back side of the PFCs (such as the heat shield). In worse case the radiative heat load to the diagnostic components like type 1 Mirnov coil presented in this paper, windows and mirrors is up to 100 kW/m^2 [4]. An important issue concerning the design of these diagnostics is to verify their suitability for steady state operation from the thermal point of view [5].

Mirnov coils are used to measure fluctuations of the magnetic field which are in particular generated by MHD modes. It is better to place the Mirnov coils as close to the plasma edge as possible because the amplitude of the magnetic fluctuations decays quickly with increasing distance from the plasma edge, which results in high thermal loads to Mirnov coils. Two types of Mirnov coils are proposed to be used in W7-X. A brief introduction of coils structure is given in Section 2. The detailed finite element (FE) thermal analysis for these two types of Mirnov coils under different load conditions were carried out to verify the design, see Section 3.

2. Types of Mirnov coils

2.1. Type 1

Type 1 (44 Mirnov coils) is to be mounted on the plasma side of the wall panel, as shown in Fig. 1. The coil former is made of Al_2O_3 and protected by the 10 mm thick graphite cap from direct exposure to plasma radiation. The coil former is a quadrate shape with dimensions of 85 mm length, 40 mm width and 14 mm high. Both the coil former and graphite cap are fixed to the stainless steel (SS) wall panel via TZM bolts. Papyex® layer (1 mm thick) is placed between the graphite cap and the wall panel as well as between the coil and the wall panel to improve thermal contact. To avoid eddy current around the coil, a thin Al_2O_3 layer is placed between the two parts of the graphite cap.

* Corresponding author at: School of Nuclear Science and Technology, University of Science and Technology of China, Jinzhai Road 96, 230026 Hefei, Anhui, PR China. Tel.: +86 18256979658.
E-mail addresses: yemy@ustc.edu.cn, myye@ipp.ac.cn (M.Y. Ye).

0920-3796/$ – see front matter © 2013 Elsevier B.V. All rights reserved.
http://dx.doi.org/10.1016/j.fusengdes.2013.05.087

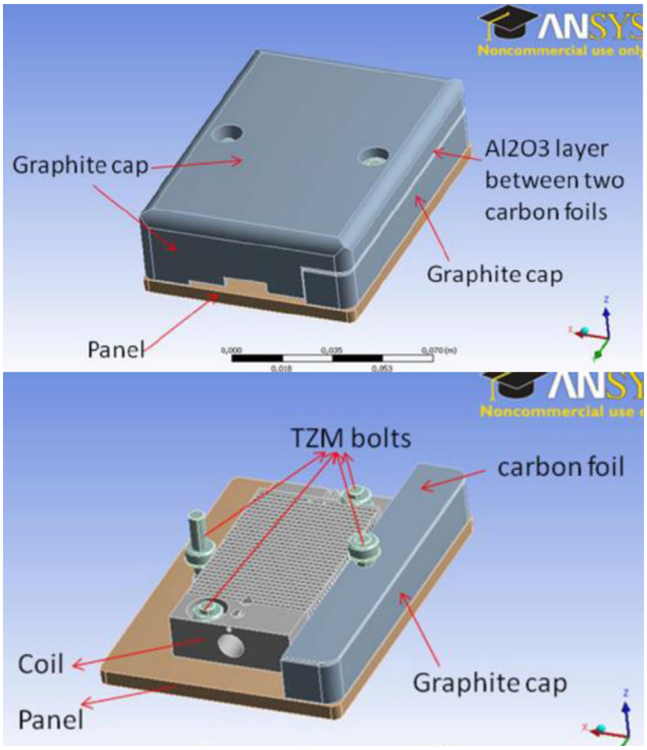

Fig. 1. Simplified 3D model of type 1 Mirnov coil mounted on the wall panel. Up: full model, down: with one part of graphite cap removed.

2.2. Type 2

Type 2 (137 Mirnov) coils will be located behind the tiles of heat shield, as shown in Figs. 2 and 3. The heat shield has graphite tile as plasma facing element bolted to CuCrZr heat sink which is brazed to a SS cooling pipe [1]. The type 2 Mirnov coils will be serially connected to the SS cooling pipe via copper support so that the coil could be actively cooled. The coil former is made of AlN and the side plates are made of Al_2O_3. In real structure the side plates do not have thermal contact with the coil former and is only inertially cooled through radiation. The coil former has a quadrate shape, with dimensions of 40 mm length, 28 mm width and 15 mm high, in the middle, and has one small quadrate ear at each of the two lateral sides. The copper support has three parts with different shape, all of which are 1 mm thick. The distance from the middle section plane of the coil former to the axes of the cooling pipes is approximately 45 mm.

3. Thermal analysis

3.1. Type 1

Type 1 Mirnov coil will be exposed to plasma radiation directly. It has to withstand heat loads as much as on the wall panel. A 3D Monte-Carlo simulation was done to investigate the thermal radiation distribution on the first wall of W7-X for 10 MW of heating power [4]. Considering W7-X will be also operated with up to 24 MW of heating power, the results gotten in numerical study was up scaled to define the load specification of wall panel [6]. The average heat load on wall panel is 100 kW/m^2 continuously and local peak heat load is 200 kW/m^2 for 10 s. Two load cases were considered for FE thermal analysis. Case 1-1: For steady state operation the heat loads of 100 and 50 kW/m^2 are assumed to the top of the graphite cap and the side faces, respectively. Case 1-2: For 10 s high power operation the heat loads of 200 and 100 kW/m^2 are assumed to the top of the graphite cap and the side faces, respectively. During normal plasma operation, the wall panel is to be cooled by 35 °C water flowing in the cooling channel with approximately 2 m/s velocity and 2 MPa pressure [2,7]. While during hot liner operation with lower plasma thermal load, the inlet water temperature is about 120 °C and the out water temperature is controlled to be not higher than 150 °C. The backside of SS wall panel is fixed at 150 °C in the FE thermal analysis. Heat transfer coefficient between the graphite cap and the wall panel as well as between the coil and the wall panel are assumed to be 2000 W/(m^2K) taking into account the effect of 1 mm layer of Papyex® [3]. Heat transmission through the ceramic gap is assumed as 1000 W/(m^2K). The heat transfer between the graphite cap and the coil is only by radiation. The materials properties for calculations of type 1 and type 2 Mirnov coils are listed in Table 1.

Fig. 4 shows the temperature distribution of the cross section of the graphite cap and the coil for Case 1-1. The minimum temperature of the graphite cap is 223 °C at the bottom of the graphite. The maximum temperature of the graphite cap is 471 °C at the side with the ceramic gap. The maximum temperature of the coil reaches up to 163 °C due to thermal radiation from the graphite cap. The temperature range of the bolt is from 282 °C at bottom to 452 °C at top. For Case 1-2, the maximum temperature and the minimum temperature of the graphite cap at 10 s reach up to 322 and 181 °C, respectively. The temperature increase of the coil is less than 2 °C (the maximum temperature of the coil is 151.3 °C). The temperature range of the bolt is from 189 °C at bottom to 275 °C at top. After switch off heat load the temperature goes back to initial value after 3 min.

Both two calculations show that the maximum temperature of graphite cap is lower than 500 °C and the temperature of the coil is

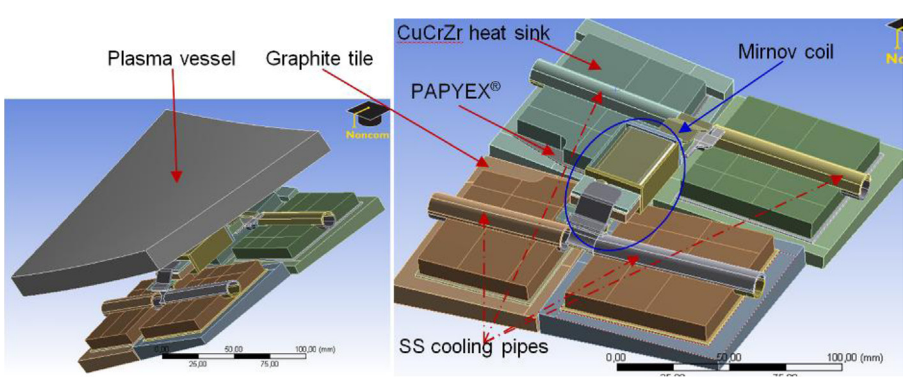

Fig. 2. 3D model of type 2 Mirnov coil with corresponding heat shield tiles and plasma vessel.

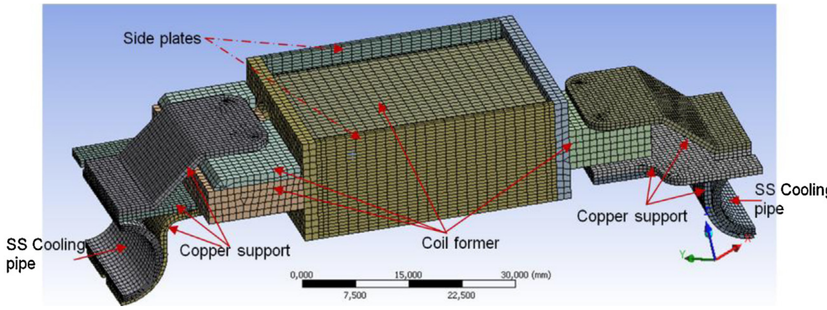

Fig. 3. FE model of type 2 Mirnov coil.

Table 1
Material properties.

Materials	Density (kg/m^3)	Specific heat (J/kg K)	Thermal conductivity (W/m K)	Emissivity
Graphite	1830	T dependent	T dependent	0.8
Stainless steel	7960	T dependent	T dependent	0.5
TZM	10150	T dependent	T dependent	0.1
Al_2O_3	3000	800	30	0.5
AlN	3200	800	170	0.5
Cu	8930	394	398	0.5
CuCrZr	8900	T dependent	T dependent	0.5

lower than 170 °C, which verified the design of type 1 Mirnov coil from the thermal point of view.

3.2. Type 2

The main thermal load on type 2 Mirnov coil is the heat radiation from visible hot surfaces of heat shield due to heat load on plasma facing side of graphite tile and the ECRH stray radiation due to non-absorbed ECRH heating power. The anticipated average heat load on heat shield tile is 250 kW/m^2 [6]. Depending on different plasma scenarios, it is possible that peak heat loads of 500 kW/m^2 would be happened in the scale of one tile due to convectional load from plasma. Two different evaluated values of ECRH stray radiation, shown in Table 2, were considered for the FE thermal analysis of type 2 Mirnov coil. As shown in Table 2, two steady state calculations were performed. Case 2-1 is with averaged heat load on heat shield tile, lower ECRH stray radiation and higher emissivity of Al_2O_3 and AlN. Case 2-2 is with peak heat load on all four heat shield tiles in the FE model, higher ECRH stray radiation, and lower emissivity of Al_2O_3 and AlN, as the worst load case.

The cooling parameters for the heat shield are the same to the ones for the wall panel except that the water velocity is approximately 6 m/s. In the FE thermal analysis of type 2 Mirnov coil, the calculated heat transfer coefficient between the SS wall of cooling pipe and the cooling water is 39330 W/(m^{2}K) based on cooling water temperature of 135 °C, velocity of 6 m/s and pressure of 1 MPa. The temperature of bottom surface of the plasma vessel is assumed at 60 °C. Heat transfer coefficient between the graphite tile and the CuCrZr heat sink, between the SS cooling pipe and the Cu support as well as between the Cu support and AlN coil former are assumed to be 2000 W/(m^{2}K) [3]. The heat transfer between different parts by radiation is considered. The bottom surfaces of the graphite tile and CuCrZr heat sink, and top surface of the plasma vessel, which are facing the coil body, are divided into many small surfaces to define a number of radiation enclosures for more accurate simulation of radiation heat transfer in the FE model.

For Case 2-1, the maximum temperature is 466 °C in the side plate, as shown in Fig. 5. The maximum temperature in the coil former and copper support is 322 and 283 °C respectively.

For Case 2-2 the calculated temperature has similar distributions with the results in case 2-1. The maximum temperature is 765 °C in the side plate. The maximum temperature in the coil former and copper support is 416 and 359 °C, respectively. Maximum temperature of the coil former of type 2 Mirnov coil in both two calculation cases is lower than 450 °C, which is acceptable.

A new design was proposed for the type 2 Mirnov coil, as shown in Fig. 6. In the new design, each coil is installed onto one cooling pipe of the heat shield tile individually, which is easier for

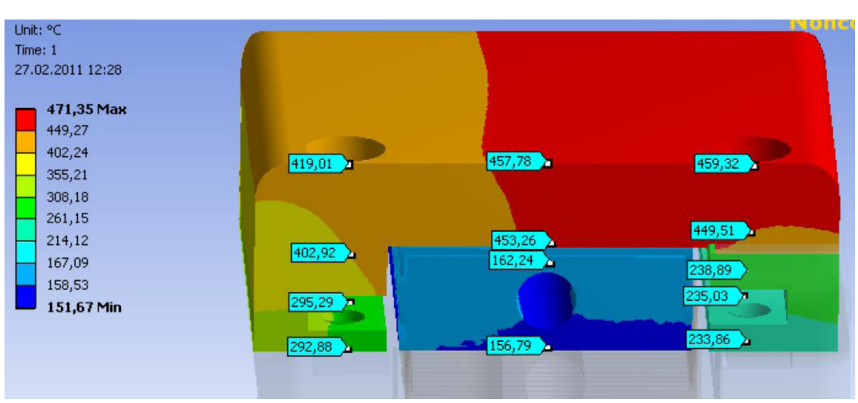

Fig. 4. Temperature distribution (°C) of the cross section of the coil and the graphite cap (case 1-1).

Table 2
Calculation cases for type 2 Mirnov coil.

Cases	Heat load on heat shield tile (kW/m^2)	ECRH stray radiation on (kW/m^2)		Emissivity of	
		AlN coil former	Al_2O_3 side plates	Al_2O_3	AlN
Case 2-1	250	9	6	0.5	0.5
Case 2-2	500	11	18	0.35	0.3

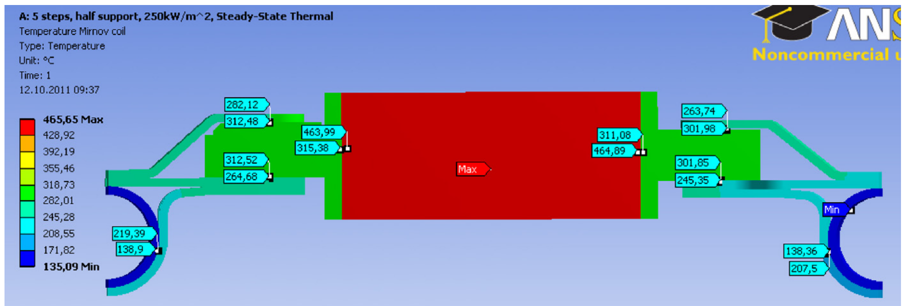

Fig. 5. Temperature (°C) distribution in type 2 Mirnov coil (case 2-1).

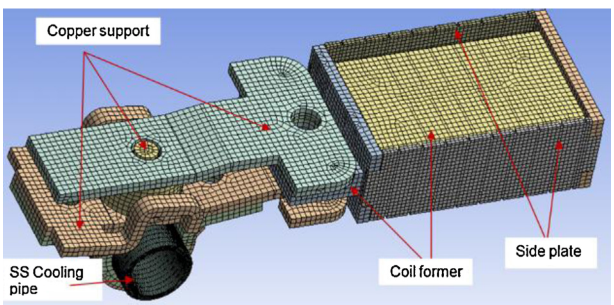

Fig. 6. Modified design of type 2 Mirnov coil.

installation and alignment. It means the coil has copper support at only one side, so the active cooling is poor compared to the former design (Fig. 3). But on the other hand, the thickness of copper support is 2 mm instead of 1 mm in the former design. Furthermore the copper support has larger contact surface with both coil former and cooling pipe. For the new design, the maximum temperature in the coil former is 458 °C under the same heat load and cooling conditions as used in calculation case 2-2, which is a little (only 8 °C) higher than the defined temperature limit (450 °C). The heat load used in case 2-2 is overestimated and not the real case since the peak heat load is only happened in the scale of one tile. The detailed location and distribution of the heat load on the heat shields are unknown and still in analysis. The further calculation for the new designed type 2 Mirnov coil would be necessary once specific heat load distribution on the heat shields is available.

4. Conclusion

FE thermal analyses for W7-X Mirnov coils under different load conditions and with different designs have been carried out. For the type 1 Mirnov coil, both steady state and transient calculations indicate the temperature in the coil structure is lower than the temperature limit. For the type 2 Mirnov coil, FE simulation results show that the first design can survive in both the normal case and the worst case. For the new proposed design of type 2 Mirnov coil with the advantage of easier installation and alignment, although the thermal analysis shows the temperature of the coil former is 8 °C higher than the temperature limit, the real case should be optimistic from the thermal point of view because heat load used in the analysis is overestimated. The further calculations for new design of type 2 will be carried out when the distribution of heat load on the heat shield is available. The Mirnov coil will be tested in the MIcrowave STray RAdiation Launch facility, MISTRAL [8] at IPP, Greifswald.

Acknowledgments

The authors would like to thank Dr. F. Schauer, Dr. J. Fellinger and Mr. V. Bykov for their discussion. This work partly supported by China National Magnetic Confinement Fusion Science Program under grant No 2011GB114000.

References

[1] R. Stadler, A. Vorkpöer, J. Boscary, A. Cardella, F. Hurd, Ch. Li, et al., Fusion Engineering and Design (2009) 305.
[2] A. Peacock, A. Girlinger, A. Vorköper, J. Boscary, H. Greuner, F. Hurd, et al., Fusion Engineering and Design 86 (2011) 1706.
[3] H. Greuner, B. Böswirth, J. Boscary, G. Hofmann, B. Mendelevitch, H. Renner, et al., Fusion Engineering and Design 66–68 (2003) 447.
[4] T. Eich, A. Werner, Fusion Science and Technology 53 (2008) 761.
[5] M.Y. Ye, M. Hirsch, R. König, M. Laux, H. Thomsen, A. Weller, et al., Fusion Engineering and Design 86 (2009) 2002.
[6] R. Brakel, M. Köppen, A. Peacock, A. Werner, M. Jakubowsk, Specification of design loads for in-vessel components of W7-X, W7-X project document, PLM: 1-AC-S0005. 0.
[7] J. Boscary, R. Stadler, A. Peacock, F. Hurd, A. Vorköper, B. Mendelevitch, et al., Fusion Engineering and Design 86 (2011) 572.
[8] D. Hathiramani, R. Binder, R. Brakel, T. Broszat, B. Brucker, A. Cardella, et al., Microwave stray radiation: measures for steady state diagnostics at Wendelstein 7-X, Fusion Engineering and Design (2013), http://dx.doi.org/10.1016/j.fusengdes.2013.01.003.